ACDIS

Research Report

Extrapolations of Global Average Temperature, Sea Level Rise, and Ocean pH Change

Chenghao Ding
Department of Nuclear, Plasma, and Radiological Engineering
University of Illinois at Urbana-Champaign

Clifford E. Singer
Program in Arms Control & Domestic and International Security
University of Illinois at Urbana-Champaign

Research of the Program in Arms Control
& Domestic and International Security

University of Illinois at Urbana–Champaign

July 2022

The research for this publication is supported by the University of Illinois. It is produced by the Program in Arms Control & Domestic and International Security at the University of Illinois at Urbana-Champaign.

ACDIS Publication Series: The ACDIS *Occasional Paper* series is designed for circulating the scholarly analytical results of faculty, students, and visiting researchers associated with ACDIS. The ACDIS *Research Reports* series publishes technical reports and findings from security related research. The ACDIS *Commentary* series serves to inform U.S. and international policy decisions. The ACDIS *International Security Policy Brief* series contains previous works with a purpose similar to those in the *Commentary* series. ACDIS *Swords and Ploughshares* contains archives of a periodic journal of collected articles aimed at a general audience. For additional information and to download publications, visit the ACDIS home page at: http://acdis.illinois.edu/

Published 2022 by ACDIS//ACDIS DIN:5.2022

University of Illinois at Urbana–Champaign 359 Armory Building, 505 E. Armory Ave.
Champaign, IL 61820-6237

Series Editor: Jazmin Tejeda

Extrapolations of Global Average Temperature, Sea Level Rise, and Ocean pH Change

CHENGHAO DING
Department of Nuclear, Plasma, and Radiological Engineering
University of Illinois at Urbana Champaign

CLIFFORD E. SINGER
csinger@illinois.edu
Program in Arms Control & and Domestic and International Security
University of Illinois at Urbana Champaign

Data-calibrated global heat and atmospheric carbon concentration equations with historically calibrated extrapolations of other contributions to radiative forcing extrapolate an additional increase in global average temperature of 2.02°C in the 101 years after 2019. Global cooperation on multiplying extrapolated anthropogenic carbon emissions to decline to nearly zero over the course of several decades limits that increase to 0.75°C. In that case, future reduction of the absolute value of a data-calibrated extrapolation of tropospheric aerosol shielding is compensated by reduction in net radiative forcing from ozone and black carbon on snow and ice. Extrapolated increase in radiative forcing from nitrous oxide is compensated by reduction in radiative forcing as accumulated carbon dioxide transports deeper into the ocean. With only 2/3 global cooperation or less, however, extrapolated global average temperature is higher and is continuing to increase in 2120. Even with complete global cooperation on an approach to zero CO_2 emissions, a slower approach that multiplies reductions by 1/2 by 2050 gives results up to 2120 that are similar to 2/3 global cooperation on faster reductions. Extrapolated sea level rise for all of these cases is similar for a century after 2120 because of an ingrained imbalance. Extrapolated estimated maximum additional loss of coral reef area for times from 2020–2120 is about three times as large with no global cooperation than with complete global cooperation. These results are not to be interpreted as predictions to answer what would actually occur, but rather as very context-dependent extrapolations that lead to interesting questions.

1. Background

This is the fifth in a series of reports describing components of a revision an earlier form [1] of the Climate Action Gaming Experiment (CAGE). The four previous reports in this series developed the inputs for the extrapolations described here. The titles of those reports are

CAGER1: Climate Action Game Experiment Motivation and Role of Radiative Forcing
CAGER2: Calibration and Extrapolation of a Simple Global Carbon Balance Model
CAGER3: Non-anthropogenic Influences on Global Average Temperature
CAGER4: Global Heat Balance Model Parameter Calibration

CAGER1 gives equations and parameters for fits to historical data needed for most of the contributions to radiative forcing used here. CAGER2 gives equations and parameters for a set of extrapolations of atmospheric concentrations $< CO_2 >$ of carbon dioxide. CAGER3 gives parameters for extrapolation of solar radiative forcing after removal of c. 11 year Schwabe cycle variations. CAGER4 gives parameters needed for extrapolation of global average temperature. Since these results are scattered amongst different documents, all of the equations and parameters needed to reproduce the results described here are collected below in Appendix B.

This report presents extrapolation results for five different approaches to future anthropogenic atmospheric carbon emissions. The starting point for each case is an extrapolation of historical emissions, accounting for future effects of depletion of resources of fluid fossil fuels as described in Appendix B and in CAGER2. Figure 1a shows the emissions multipliers for each of these five cases. The curve labeled 1 Green Deal corresponds to global cooperation with progress to nearly zero emissions after fifty years. The other curves labelled Green Deal multiply the 1 Green Deal

emissions limitation factors by the numbers indicated on Figure 1a. The 1/3 and 2/3 curves are included to explore incomplete global cooperation that prevents an expeditious approach to emissions limits proceeding all of the way to nearly zero emissions. The curve labelled Soft does approach zero emissions, but not as expeditiously as for the faster reductions in the 1 Green Deal case.

Figure 1b shows the $< CO_2 >$ paths that correspond to the five curves in Figure 1a. Figures 2a and 2b respectively show the corresponding radiative forcing from $< CO_2 >$, and from all of the extrapolated sources combined. Figure 2b shows that total radiative forcing for the full Green Deal case stays steady for the last few decades of the coming hundred years. This is despite continuing growth of forcing from nitrous oxide shown in Figure 3a. A reason for this is that forcing from $< CO_2 >$ continues to decline as that part of the CO_2 that had accumulated in the atmosphere gradually transitions into non-atmospheric locations as it approaches being nearer to equilibrium with exchangeable carbon in those locations.

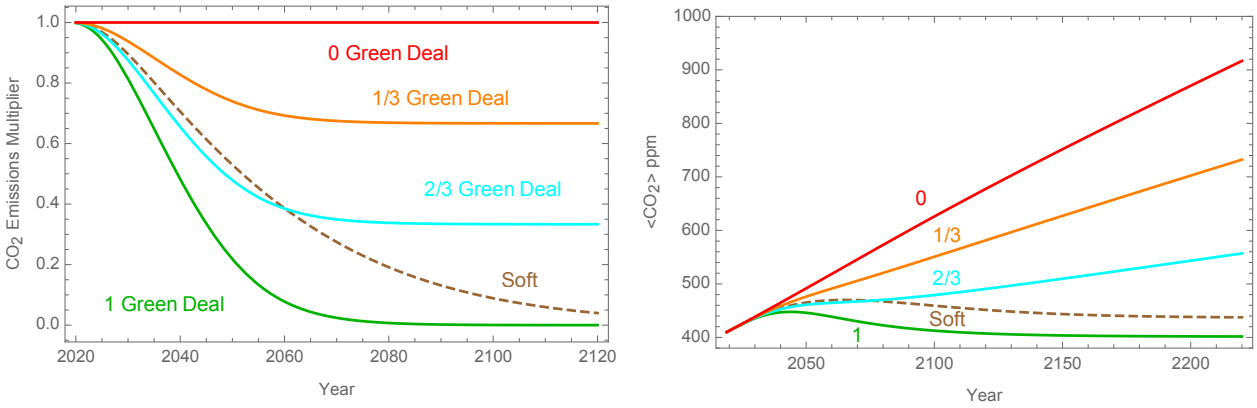

Figure 1. (a) Multipliers of extrapolated global anthropogenic atmospheric carbon emissions, and (b) corresponding evolutions of atmospheric CO_2 concentration.

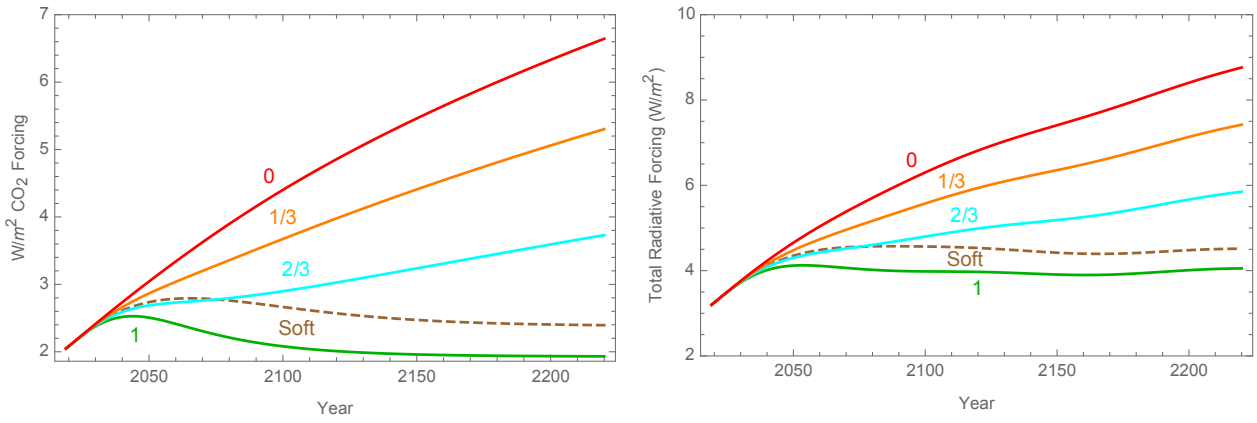

Figure 2. (a) Radiative forcing from CO_2 and (b) total radiative forcing corresponding to $< CO_2 >$ evolutions in Figure 1b.

Meanwhile, the sum of solar, halogen, land use change (LUC), methane, and stratospheric water vapor forcing stays about constant, as indicated in Figure 3a. In particular, halogen forcing, LUC forcing, and methane emissions are fit with logistic functions. Methane has a short atmospheric lifetime of about nine years, so its atmospheric concentration and radiative forcing level off with

about a decade's lag as its logistic function emissions rate levels off. Forcing from stratospheric water vapor is proportional to the concentration $< CH_4 >$ with a short lag and also levels off. Also, the solar forcing used has comparatively small amplitude 87.5-year Gleissberg cycle oscillations around a very slowly evolving multicentury-scale change.

Moreover, the sum of data-calibrated short-lived contributions to net forcing from regionally dependent pollutants shown in Figure 3b has a slightly declining trend starting about 2070 that just about cancels other contributions to radiative forcing to about to about level off the sum of all the contributions to radiative forcing for the full Green Deal case in Figure 2b.

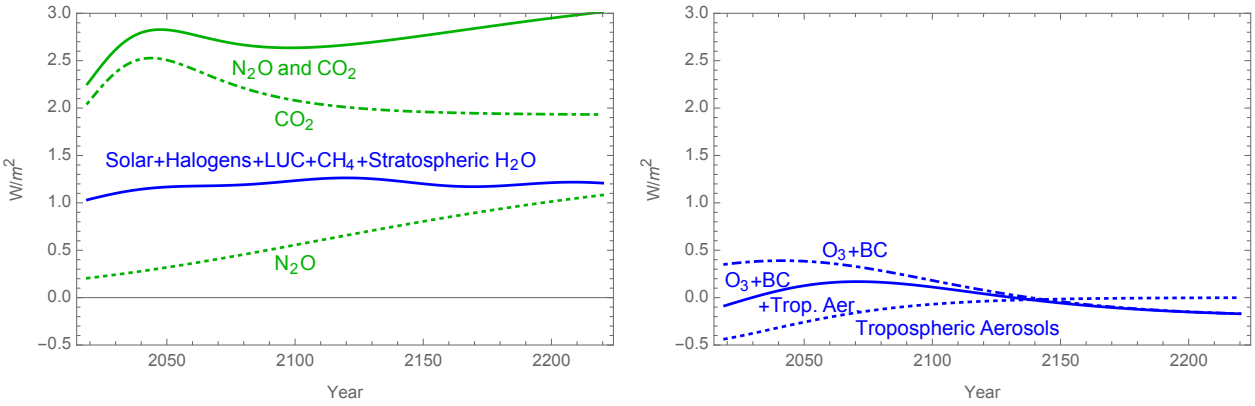

Figure 3. (a) Radiative forcing from N_2O (dotted curve), from CO_2 (dot-dashed curve), and from both together, (upper solid curve). The lower solid curve shows the sum and from solar forcing excluding Schwabe cycle variations, from halogens, from land use changes with their effect on albedo, CH_4, and stratospheric water vapor. (b) Radiative forcing from tropospheric aerosols (dotted curve), from the combination of ozone and black carbon on snow and ice (dot-dashed curve), and from these together (solid curve).

However, for the 1/3 and 2/3 Green Deal cases, the rise of $< CO_2 >$ forcing plotted in Figure 2a is too strong to allow stabilization of overall total radiative forcing. For the Soft case, the $< CO_2 >$ forcing does eventually decline, but the extrapolated total radiative forcing remains 0.56 W/m^2 higher than the 1 Green Deal case even in 2120.

2. Temperature, Sea Level, and Upper Ocean Acidity

2.1. **Temperature.** Figure 4a plots extrapolations of temperature differences from a 1986–2005 temporal and global average temperature reference value. The CAGER4 estimate of the difference between that 1986–2005 average and a transient-corrected global average temperature in equilibrium with zero radiative forcing is 0.8 °C. As described in CAGER4, after accounting for methodology differences including how effects of the 1991 Pinatubo volcanic eruption are handled, that 0.8 °C increment is close to another estimate [3] of the 1986–2005 average temperature over a 1750 using a set of global circulation models instead of the global heat balance equation used here.

The global average temperatures plotted in Figure 4a are averaged over c. 11 year Schwabe cycle variations in solar irradiance and over variations correlated with the El Niño Southern Oscillation. Variations of stratospheric aerosol shielding from volcanoes with shielding less than twice as strong as the post-1836 average are assumed to average to zero. The results plotted in Figure 4a are designed for subsequent use in an analysis based on future changes in the parameters plotted herein, averaged over small transient variations and in the absence of future stratospheric aerosol injections that have enduring global economic impact. These extrapolations are thus not directly

comparable to results from other approaches that include large transient stratospheric aerosols or repeating variations or short-term oscillations of either anthropogenic or non-anthropogenic origin.

Only the cases shown in Figure 4a that eventually lead to zero anthropogenic atmospheric carbon emissions prevent a continuing rise in global average temperature after 2120. For the full Green Deal case in Figure 4a, the temperature increase from 2019 to a maximum in 2077 is 0.77°C. After 2070, extrapolated temperature is nearly constant, declining by 0.02°C from 2077 to 2120. For the 2/3 Green Deal case, the increase in temperature from 2019 to 2120 is 1.20°C. The Soft Green Deal temperature curve is slightly above but nearly equal to the 2087 2/3 Green Deal case, crossing it in 2085 and then declining in 2120 to 1.04°C above the 2019 value. Using a data-calibrated discount rate of 0.023/yr [1, 5], the weight of future financial impacts of a given change in economic productivity declines by half every 30 years. In that context, the Soft and 2/3 Green Deal extrapolations may be functionally nearly equivalent with respect to differences in the net present value of economic impacts of climate change.

The 0 and 1/3 Green Deal results plotted in Figure 4a eventually lead to future extrapolated temperature increases over the year 2019 value that are over twice as large as for the full Green Deal case. For the 1/3 and 0 Green Deal cases, the temperature increases from 2019 to 2120 are respectively 1.62 and 2.02°C, compared to 0.75°C for the full Green Deal case. However, there are smaller temperature differences between the 0 and full Green Deal cases of 0.10°C and 0.58°C at 30 and 60 years after 2019 respectively. Would an expectation of the growth in that difference over the second thirty year interval be enough to prompt a near-term launch and subsequent expeditious implementation of a comprehensive global plan to implement a full or very nearly full Green Deal as described here? That is a question for work in progress at the time of this writing.

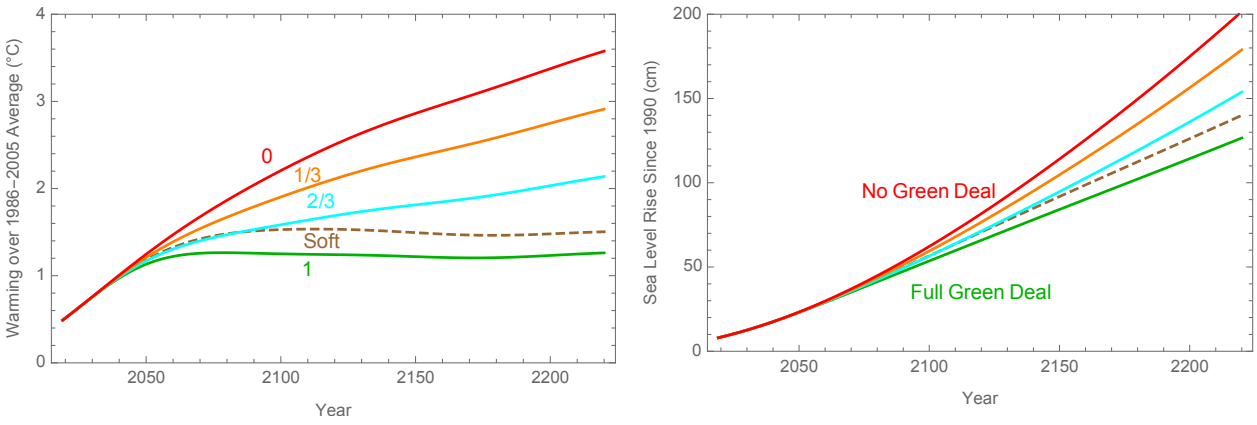

Figure 4. (a) Global average temperature difference from a 1951–1980 average and (b) global average sea level rise from 1990, both with radiative forcing extrapolations in Figure 2b.

2.2. **Sea Level.** Figure 4b plots results of solving an equation for global average sea level S of the form

$$H' = a_S(\tau - \tau_S) \tag{2.1}$$

H is the change in sea level in centimeters since 1990, and τ is global average temperature difference from an equilibrium temperature with 1745–1755 average radiative forcing. Values of the parameters $a_S = 0.322$ and $\tau_S = 0.162$°C were calibrated against historical data [6] as described below in Appendix A.

The two solid curves in Figure 4b between the No and Full Green Deal curves correspond to the 1/3 and 2/3 Green Deal cases in Figure 4a. The dashed curve corresponds to the Soft Green Deal

case in Figure 4a. As noted in Appendix A, this simple model provides a good fit to post-World-War-II estimates of changes in global mean sea level, but it does not attempt separately model several processes [6] that affect that level.

In the context of this model, sea level rise increases even if global average temperature levels off, as long as it levels off at a temperature higher than the temperature in which it would be in equilibrium as determined by the parameter τ_S. An alternative approach [7] has sea level eventually reaching an equilibrium at a higher temperature, albeit on a time scale of two centuries or more that is long compared to the results plotted in Figure 4b and thus not of particular interest here. The results shown in Figure 4b are only meant as an empirical indication of the magnitude of possible future sea level rise, rather than as a systematic attempt at extrapolation based on models of the underlying physical process.

2.3. **Upper Ocean Acidity and Coral Reef Loss.** Figure 5a shows extrapolations of changes in surface ocean layer acidity corresponding to the $< CO_2 >$ extrapolations in Figure 1b. Estimates of the impact of the change in pH from 1750 on the fraction of total global coral reef area compared to 1750 are plotted in Figure 5b. The formulas used [8] for Figure 5a and 5b are respectively

$$\Delta_{pH} = \alpha_H (< CO_2 > -280)^{\beta_H} \tag{2.2}$$

with $\alpha_H = 0.00569$ and $\beta_H = 0.67$; and

$$f = \gamma_H \, \Delta_{pH} / (1 + \gamma_H \, \Delta_{pH}) \tag{2.3}$$

with $\gamma_H = 0.56$.

The plots in Figure 5b account only for the effect of changes in pH, not for possible additional changes driven by increases in temperature. The latter could ideally be compensated for by re-seeding coral with species adapted to a higher temperature, but that could prove to be impractical. The dashed portions of the curves in Figure 5b could only be reached if natural or artificial reseeding succeeded quickly enough once acidity peaked and declined, which could be problematic in practice.

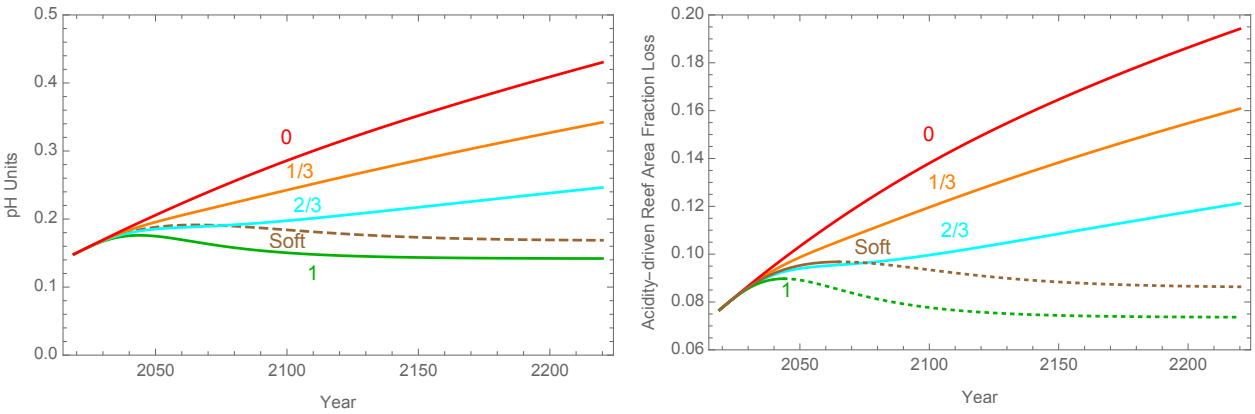

Figure 5. (a) Change in surface ocean layer pH since 1750 and (b) extrapolated acidity-driven fractional global loss of coral reef area since 1750, both with $< CO_2 >$ evolutions as in Figure 1b.

Evolution of changes in $< CO_2 >$, global average temperature, sea level, and coral reef damages since 1990 are needed for future use in an economic impact model along the lines of the FUND model [9]. It is for this reason that results for extrapolations of all of these quantities have been developed as described here.

Appendix A. Sea Level

Figure 6 compares estimates of the difference in global mean sea level from its 1980–1999 average to a least squares fit to the solution from 1946–2015 of the equation $H' = a_S(\tau - \tau_S)$. The initial condition in 1946 with the least squares fit is -4.28 cm, which is 0.21 cm over the first data point. This result suggests that global average temperature could need to be reduced to levels below that before World War II in order for sea level increases to stop.

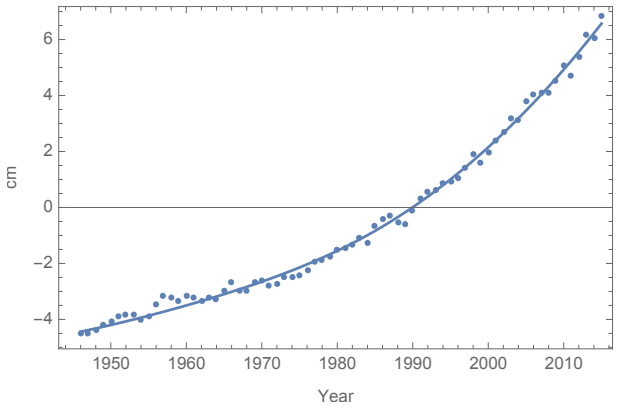

Figure 6. Difference in global mean sea level from its 1980–1999 average (dots) compared to a least squares fit to solutions of the equation $H' = a_S(\tau - \tau_S)$ with $H = -4.50$ cm in 1946 as the initial condition.

Determinants of global mean sea level include thermal expansion, land ice melts, changes in regional wind patterns, and a small effect from terrestrial water storage [6]. The results shown in Figure 6 lump all of these together to give a result that couples increases of global mean seal level with increasing global average temperature in a matter empirically consistent with seven decades of observational data. A more complete model than that adopted here uses an equation of the form $dH/dt = a(\tau - \tau_{ref} - \tau_s) + b\, d\tau/dt$, with the last term accounting separately for thermal expansion [10]. Using a data set with temperature growing exponentially, the three parameters in this equation cannot be determined independently, so the simpler form without that additional term is used here. A more complex model suggests that the thermal inertia component of sea level rise by the end of the twenty-first century would be significant but substantially smaller than the total rise in sea level [11]. While a near-term increase in global mean sea level seems likely to continue as global average temperature increases, how that trend would work out quantitatively in the much longer term with the various extrapolated evolutions of temperature plotted in Figure 5a is not a question that is addressed here.

Appendix B. Equations and Parameters

Parameters for atmospheric emissions and radiative forcing are listed in Table 1. The first five rows of numbers Table 1 list parameter sets for anthropogenic atmospheric emissions of nitrous oxide, methane, and carbon in CO_2. Initial concentrations in 1750 of $< N_2O >$ and $< CH_4 >$ in ppb are respectively 270.6 and 788.2. Parameters used to convert extrapolations of those emissions to atmospheric concentrations and radiative forcing are listed in Tables 2 and 3. The rest of Table 1 lists sets of parameters used to extrapolate radiative forcing from some other sources. Only one constant b_0 is needed to make the sum of the three cosinusoidal contributions to solar radiative equal plus that constant equal to 0 in 1750, and only that sum is used here.

Table 1. Emissions and Radiative Forcing Parameters

Type	$u = 1/(e^{-(t-b_2)/b_3})$	b_0	b_1	b_2	b_3
Emissions	Formula	ppb/yr	ppb/yr	Julian Year	yr
N_2O	$b_0 + b_1 u$	-0.01	4.95	2059.82	50.76
CH_4	”	-0.07	135.21	1954.50	27.03
Carbon	Formula	TtonneC/yr	TtonneC/yr	Julian Year	years
Industrial	$b_0 + b_1 u$	-0.000002	0.01529	2002.57	27.82
Land Use Early	$b_0 + b_1 u(1-u)$	-0.000076	0.00594	1950.98	46.20
Land Use Late	$b_1 u(1-u)$	0	0.00297	2021.63	8.91
Anthropogenic Forcing	Formula	W/m^2	W/m^2	Julian Year	yr
Halogens	Max[$b_0 + b_1 u$,0]	-0.002	0.405	1979.83	7.41
Land Use Changes	$b_0 + b_1 u$,	0.002	-0.213	1916.49	35.96
Contrails	Max[$b_0 + b_1 u$,0]	-0.002	0.234	2040.36	20.15
O_3 +BC on Snow/Ice	$b_0 + b_1 u(1-u)$	-0.206	2.383	2041.44	42.99
AR6 Tropos. Aerosol	”	0.003	-5.423	1994.81	32.11
Solar Forcing	Formula	W/m^2	W/m^2	Julian Year	yr
Grand Minimum	$b_1 \cos[2\pi(t-b_2)/b_3]$	0	-0.046	1650	842
Gleissberg	”	0	0.032	1772.23	87.53
Triple Gleissberg	$b_0 +$ ”	0.023	-0.020	1927.00	269.95

Note that the long-term limit of $b_1/(1-u)$ is b_1, while the maximum value of $b_1 u(1-u)$ is $b_1/4$. This should be kept in mind when comparing the values of b_1 in Table 1 for tropospheric aerosols and for ozone plus black carbon on snow to the values of b_1 for the other contributions to radiative forcing listed in Table 1. Also, fitting parameters in Table 2 for tropospheric aerosol forcing are based on figure 2.10 of the Working Group 1 contribution to the Sixth Assessment Report (AR6) of the Intergovernmental Panel on Climate Change [12]. Table 3 lists a factor $c_a = 0.371$ that multiplies the AR6 radiative forcing from tropospheric aerosols for production of the results shown in the present report.

Parameters and equations for radiative forcing as functions of $< N_2O >$, $< CH_4 >$, and $< CO_2 >$ are listed in Table 2. The atmospheric concentrations G of gases $< N_2O >$, $< CH_4 >$ needed for the radiative forcing formulas in Table 2 can by computed by numerical integration of $G' = S_G - G/t_G$. The extrapolated emissions sources S_G are to be computed using the numbers listed in Table 1. The atmospheric lifetimes t_G for nitrous oxide and methane are listed in Table 3. An alternative described in CAGER1and used here is analytic solution using a hypergeometric function.

Additional parameters used to produce the results in the present report are listed in Table 3. The last four parameters listed in Table 3 specify the multipliers of extrapolated anthropogenic carbon emissions used above. (The Soft Green Deal case has $g_2 = 24$ years instead 8 years for the other cases plotted in the figures above.) The multipliers $1 - g_1 + g_1 f_p/f_{p0}$ for extrapolated anthropogenic atmospheric carbon emissions have f_{p0} equal to the value of f_p for $y = t - 2019 = 0$, where

$$f_p = (f_{45} - f_{23})y + g_3(1 + f_{23}) \ln[e_{y3} + e_{23}] - g_5(1 + f_{45}) \ln[e_{y5} + e_{45}] \tag{B.1}$$

with $e_{23} = e^{g_2/g_3}$, $e_{45} = e^{g_4/g_5}$, $e_{y3} = e^{y/g_3}$, $e_{y5} = e^{y/g_5}$, $f_{23} = 1/e_{23}$, and $f_{45} = 1/e_{45}$. The values of f_p/f_{p0} at $y = 0$ and as $y \to \infty$ are respectively 1 and 0. So, the initial and long-term limits of

$1 - g_1 + g_1 f_p / f_{p0}$ are respectively 1 and $(1 - g_1)$. The form of $f'_p = df_p/dy$ is of one smoothed step followed by another smoothed step function that eventually cancels the step from the earlier step.

Table 2. Radiative Forcing Formulas

j	1	2	3
a_j	-2.4785×10^{-7}	-3.4197×10^{-4}	-8.9603×10^{-5}
a_j units	W m^{-2} ppm^{-2}	W m^{-2} ppm$^{-1/2}$	W m$^{-1/2}$ ppb^{-1}
b_j	7.5906×10^{-4}	2.5455×10^{-4}	-1.2462×10^{-4}
b_j units	W m^{-2} ppm^{-1}	W m^{-2} ppb$^{-1/2}$	W m^{-2} ppb$^{-1/2}$
c_j	-2.1492×10^{-3}	-2.4357×10^{-4}	0
c_j units	W m^{-2} ppb$^{-1/2}$	W m^{-2} ppb$^{-1/2}$	
d_j	5.2488	0.12173	0.045194
d_j units	W m^{-2}	W m^{-2} ppb$^{-1/2}$	W m^{-2} ppb$^{-1/2}$
$\{C_0, M_0, N_0\}$	277.15 ppm	731.41 ppb	273.87 ppb

$F_C = (d_1 + a_1(C - C_0)^2 + b_1(C - C_0) + c_1\sqrt{N})\ln(C/C_0)$
$F_N = (a_2\sqrt{C} + b_2\sqrt{N} + c_2\sqrt{M} + d_2)(\sqrt{N} - \sqrt{N_0})$
$F_M = (a_3\sqrt{M} + b_3\sqrt{N} + d_3)(\sqrt{M} - \sqrt{M_0})$

Table 3. Equations and Additional Parameters

Symbol	Units	Value	Description
t_{N_2O}	yr	116	$< \mathrm{N_2O} >' = e_{N_2O} - < \mathrm{N_2O} > / t_{N_2O}$
t_{CH_4}	yr	9.1	$< \mathrm{CH_4} >' = e_{CH_4} - < \mathrm{CH_4} > / t_{CH_4}$
a_H	$(\mathrm{W/m^2})$ /ppb	0.000048	$F_{H_2O} = a_H < \mathrm{CH_4} >\|_{t-t_{lag}}$
t_{lag}	yr	2	$< \mathrm{CH_4} >$ lag for stratospheric $\mathrm{H_2O}$ forcing
$< \mathrm{N_2O} >_{2019}$	ppb	331.8	$< \mathrm{N_2O} >$ fit at t=2019
$< \mathrm{CH_4} >_{2019}$	ppb	1871.8	$< \mathrm{CH_4} >$ fit at t=2019
a_{2019}	TtonneC	0.872	Carbon content in 2019 for $a' = f_e e_c - s'$
s_{2019}	TtonneC	1.076	Equilibrating reservoir 2019 fit for $s' = \nu(r_{sa} a - s)$
ν	1/yr	0.01285	Carbon reservoirs equilibration rate
r_{sa}	1	1.533	s/a ratio in equilibrium
f_m	1	0.581	Minimum prompt sequestration escape fraction f_e
a_{1750}	TtonneC	0.592	Parameter in $f_e = 1 + (f_m - 1)e^{(a - a_{1750})/a_3}$
a_3	TtonneC	0.524	Parameter for f_e
f_{coal}	1	0.41	$e_c = f_{coal} e_{ind} + (1 - f_{coal}) f_d e_{ind} + e_{land}$
b_d	1	0.68	Depletion factor $f_d = ((1 + b_d U)/(1 + b_d U_{2019}))^{\beta_f}$
U_{2019}	TtonneC	0.44	Cumulative industrial carbon emissions in 2019
β_f	1	-0.35	Fluid fossil fuel depletion elasticity exponent
τ_{2019}	°C	1.309	Temperature increase from 1750 to 2019
β	°C $/(\mathrm{W/m^2})$	0.518	Climate sensitivity in $c_{th}\tau' = F - \tau/\beta$
c_{th}	$(\mathrm{W/m^2})$yr/°C	28.49	Thermal inertia parameter
c_a	1	0.371	Efficacy of AR6 tropospheric aerosol forcing
H_{2019}	cm	8.14	2019 increase in sea level from 1980–1999 average
a_S	(cm/yr)/°C	0.349	Coefficient in $H' = a_S(\tau - \tau_S)$
τ_S	°C	0.162	Temperature for $H' = 0$
α	pH $\mathrm{ppm}^{-\beta}$	0.00569	$\Delta_{pH} = \alpha(< \mathrm{CO_2} > - 280)^{\beta}$
β	1	0.67	pH formula exponent
γ	1/pH	0.56	Coral reef loss fraction $= \gamma\Delta_{pH}/(1+\gamma\Delta_{pH})$
g_1	1	1	Reference Green Deal emissions reductions fraction
g_2	30	yr	Time scale for emissions multiplier reductions
g_3	8	yr	Reference case gradual approach to final reductions
g_4	4	yr	Emissions limits initial delay
g_5	4	yr	Timescale for reductions phase-in

References

[1] Singer, C. and L. Matchett, 2015. Climate action gaming experiment: Methods and example results, *Challenges* **6**, 202–228, doi:10.3390/challe6020202.

[2] Ding, C., and C. Singer. 2022. University of Illinois at Urbana-Champaign Program in Arms Control & Domestic and International Security Research Reports ACDIS//ACDIS DIN:1, Climate Action Game Experiment motivation and role of radiative forcing; DIN:2, Calibration and extrapolation of a simple global carbon balance model; DIN:3, Non-anthropogenic influences on global average temperature; DIN:4, Global heat balance model parameters,; https://acdis.illinois.edu/outreach/research/research-reports.

[3] Hawkins, E., P. Ortega E. Suckling, A. Schurer, G. Heferl, P. Jones, M. Joshi, T. Osborn, V. Masson-Delmotte, J. Mignot, P. Thorne, and G. van Oldenborgh. 2017. Estimating changes in global temperature since the preindustrial period, *Bulletin of the American Meteorological Society*, 98, 1841–1856, https://doi.org/10.1175/BAMS-D-16-0007.1.

[4] GISTEMP Team. 2021. *GISS Surface Temperature Analysis (GISTEMP), version 4.* NASA Goddard Institute for Space Studies, https://data.giss.nasa.gov/gistemp/; https://data.giss.nasa.gov/gistemp/tabledata_v4/GLB.Ts+dSST.csv, accessed December 22, 2021.

[5] Singer, C. E., T. S. Rethinaraj, S. Addy, D. Durham, M. Khanna, B. Kuehl, J. Luo, W. Quimio, K. Rajendran and D. Ramirez , J. Qiang, J. Scheffran, T. N. Tiouririne, and J. Zhang, 2008. Probability distributions for carbon emissions and atmospheric response, *Climatic Change* **88**, 309–342, https://doi.org/10.1007/s10584-008-9410-4.

[6] Dangendorf, S., C. Hay, F. M. Calafat, M. Marcos, C. Piecuch, K. Berk, and J. Jensen. 2019. Persistent acceleration in global sea-level rise since the 1960s, *Nature Climate Change* **9**, 705–710, https://doi.org/10.1038/s41558-019-0531-8.

[7] Grinsted, A., J. Moore, and S. Jevrejeva. 2010. Reconstructing sea level from paleo and projected temperatures, 200–2100 AD, *Climate Dynamics* **34**, 311–472.

[8] Brander, L., K. Rehdanz, R. Tol, P. Beukering, and J. van Pieter. 2009. The economic impact of ocean acidification on coral reefs, ESRI Working Paper No. 282, The Economic and Social Research Institute (ERSI), Dublin, http://hdl.handle.net/10419/28758, accessed May 20, 2019.

[9] Anthoff, D., and R. S. J. Tol, 2014. The climate framework for uncertainty, negotiation and distribution (FUND), technical description, version 3.9, http://www.fund-model.org/versions, accessed May 18, 2019.

[10] Vermeer, M., and S. Rahmstorf. 2009. Global sea level linked to global temperature, *Proceedings of the National Academy of Science* **106**, 21527–21532, https://doi.org/10.1073/pnas.0907765106.

[11] Vega-Westhoff, B., R. L. Sriver, C. A. Hartin, T. E. Wong, K. Keller, Impacts of observational constraints related to sea level on estimates of climate sensitivity, Earth's Future **7**, 677-690, https://doi.org/10.1029/2018EF001082, 2019.

[12] IPCC, 2021. *Climate Change 2021: The Physical Science Basis. Contribution of Working Group I to the Sixth Assessment Report of the Intergovernmental Panel on Climate Change*, V. Masson-Delmotte, P. Zhai, A. Pirani, S. L. Connors, C. Pèan, S. Berger, N. Caud, Y. Chen, L. Goldfarb, M. I. Gomis, M. Huang, K. Leitzell, E. Lonnoy, J. B. R. Matthews, T. K. Maycock, T. Waterfield, O. Yelekçi, R. Yu and B. Zhou (eds.). Cambridge University Press. In Press, https://www.ipcc.ch/report/sixth-assessment-report-working-group-i/.